Inferring phenotypic plasticity and population responses to climate across tree species ranges using forest inventory data

Running title: Understanding phenotypic variation in natural populations

Thibaut Fréjaville[1*], Bruno Fady[2], Antoine Kremer[3], Alexis Ducousso[3], Marta Benito Garzón[1]

[1] *BIOGECO (UMR 1202), INRA, Univ Bordeaux, 33615 Pessac, France*

[2] *INRA, UR629, Ecologie des Forêts Méditerranéennes (URFM), 84914 Avignon, France*

[3] *BIOGECO (UMR 1202), INRA, Univ Bordeaux, 33610 Cestas, France*

[*] *Correspondence author. E-mail: thibaut.frejaville@gmail.com*

Acknowledgements

This publication is part of a project that has received funding from the "Investments for the Future" program IdEx Bordeaux (ANR-10-IDEX-03-02) and the European Union's Horizon 2020 research and innovation programme under grant agreement No. 676876 (GenTree). We are very grateful to Juan Fernandez Manjarrés (CNRS-Université Paris-Sud) with whom the discussion about how to use NFI for splitting genetic and plastic effects started many years ago. We are indebted to Denis Vauthier and Franck Rei (INRA UEFM, Avignon), Fabrice Bonne, Thierry Paul and Vincent Rousselet (INRA UEFL, Nancy) and Jean Gauvin (INRA UGBFOR, Orléans) for data collection in the *Abies alba* provenance tests. We acknowledge colleagues from different European institutions for providing access and use of provenance data in *Quercus petraea*: Jon Kehlet Hansen, University of Copenhagen, for Denmark; Brigitte Musch and the staff of the French Office National des Forêts for France; Hans-Martin Rau, Jochen Kleinschmit, Josef Svolba of Niedersächsische Forstliche Versuchsanstalt, Abteilung Forstpflanzenzüchtung, Staufenberg, Escherode and Wilfried Steiner, Alwin Janssen, Nordwestdeutsche Forstliche Versuchsanstalt, Abteilung Waldgenressourcen, Hann-Münden, for Germany; Władysław Chałupka, Henryk Fober of the Instytut Dendrologii PAN, Kórnik for Poland; Steve J Lee, Alan M. Fletcher and Edward P. Cundall, Northern Research Station, for the United Kingdom.

ABSTRACT

Aim: To test whether intraspecific trait responses to climate within and among populations across species distribution ranges can be untangled using field observations, under the rationale that, in natural forest tree populations, long-term climate shapes local adaptation of populations while recent climate change drives phenotypic plasticity.

Location: Europe.

Time period: 1901-2014.

Taxa: Silver fir (*Abies alba* Mill.) and sessile oak (*Quercus petraea* (Matt.) Liebl.).

Methods: We estimated the variation of individual tree height as a function of long-term and short-term climates to tease apart provenance effects (variation among populations of different geographical origin), plasticity (within population) and their interaction, using mixed-effect models calibrated with National Forest Inventory data (*in-situ* models). To validate our approach, we tested the ability of *in-situ* models to predict independently tree height observations in common gardens where provenance and plastic effects can be measured and separated. *In-situ* model predictions of tree height variation among provenances and among planting sites were compared to observations in common gardens and to predictions from a similar model calibrated using common garden data (*ex-situ* model).

Results: In *Q. petraea*, we found high correlations between *in-situ* and *ex-situ* model predictions of provenance and plasticity effects and their interaction on tree height ($r > 0.80$). We showed that the *in-situ* models significantly predicted tree height variation among provenances and sites for *Abies alba* and *Quercus petraea*. Spatial predictions of phenotypic plasticity across species distribution ranges indicate decreasing tree height in populations of warmer climates in response to recent anthropogenic climate warming.

Main conclusions: Our modelling approach using National Forest Inventory observations provides a new perspective for understanding local adaptation to climate and phenotypic plasticity across species ranges. Its application is particularly interesting for species for which common garden experiments do not exist or do not cover the entire climatic range of the species.

Keywords: *Abies alba*, common gardens, intraspecific trait variation, national forest inventory, *Quercus petraea*, tree height

INTRODUCTION

Understanding the causes of phenotypic variation across species distribution ranges is important because phenotypic traits are fundamental drivers of community assembly, ecosystem functioning, and population response to climate change (Diaz *et al.*, 2004; Shipley *et al.*, 2006; Alberto *et al.*, 2013; Kunstler *et al.*, 2016). Phenotypic variation within and among populations are the two components of intraspecific trait responses to environmental factors. Traits vary within populations according to phenotypic plasticity (i.e., the capacity of one genotype to render different phenotypes under different environments, Valladares *et al.*, 2006), and among populations according to local adaptation (i.e., the fact that individuals have a better fitness in their local environment than individuals from other populations, Kawecki & Ebert, 2004) in addition to neutral and maladaptive components of genetic variation (Savolainen *et al.*, 2007; Leimu & Fischer, 2008). The spatial distribution of the amount of phenotypic variation that can be attributed to phenotypic plasticity or to local adaptation may change the response of organisms to climate change as predicted by theoretical approaches (Chevin *et al.*, 2010; Valladares *et al.*, 2014). Yet, attributing the cause of trait-climate relationships across species ranges to among and within population components remains a challenge without using costly, long-term common garden experiments (Benito Garzón *et al.*, 2019).

Long-term spatial divergence under different climatic conditions is known to promote phenotypic differentiation of populations as a result of local adaptation to climate (Mimura & Aitken, 2010; Savolainen *et al.*, 2013; Yeaman *et al.*, 2016), which affects their current response to a particular climate (Rehfeldt *et al.*, 2002; Savolainen *et al.*, 2007; Valladares *et al.*, 2014). However, significantly less is known about the distribution of phenotypic plasticity and its importance for populations for coping with rapid climate change across the species range, especially in long-lived sessile organisms such as forest trees (Nicotra *et al.*, 2010; Benito Garzón *et al.*, 2011; Valladares *et al.*, 2014; Duputié *et al.*, 2015).

Patterns of phenotypic plasticity and local adaptation of populations have long been assessed using common garden or reciprocal transplant experiments (also named ‘provenance tests’ or ‘genetic trials’), in which genotypes of known climatic origin (i.e., provenances) are growing in experimental plantations where short-term environmental conditions are controlled. In common gardens, trait differences among provenances that are related to the long-term climate of origin of the provenance are often interpreted in terms of local adaptation (e.g. Mimura & Aitken, 2010; Savolainen *et al.*, 2013; Benito Garzón *et al.*, 2019), although neutral and maladaptive components of genetic variation may also be responsible for differences among provenances (Savolainen *et al.*, 2007; Leimu & Fischer, 2008). On the other hand, plasticity is quantified by trait variation with the short-term climatic conditions at the planting sites (see Matyas, 1994; Wang *et al.*, 2006; Leites *et al.*, 2012 for forest trees). Common gardens have been established for a few economically important tree species for which only a restricted range of populations and ontogenic stages have been studied, which makes the understanding of phenotypic variation across species ranges limited (Fady *et al.*, 2016).

On the other hand, causes of phenotypic variation are confounded in natural conditions, in addition to the effects of ontogeny and competition. National Forest Inventories (NFI) provide extensive data of phenotypic variation of forest trees in natural conditions, and hence, they have been widely used to test different ecological questions such as the effects of functional traits on competition, forest productivity and response to climate change (Kunstler *et al.*, 2016; Ratcliffe *et al.*, 2016; Ruiz-Benito *et al.*, 2017), but to date, how phenotypic traits in NFI vary as a function of differences among provenances and plasticity remains unexplored.

Here we show that intraspecific trait variation among provenances, species plasticity and their interaction, can be statistically estimated using the field data recorded in French NFI for two ecologically and economically important forest tree species usually managed using natural regeneration, *Abies alba* Mill. and *Quercus petraea* (Matt.) Liebl. We use tree height, an important adaptive and fitness-related trait (Savolainen *et al.*, 2007; Díaz *et al.*, 2016), to independently test our approach on field observations (NFI) and we validate our findings using common garden data. Our approach expands the space-for-time substitution analysis developed in common gardens (Matyas, 1994; Rehfeldt *et al.*, 2002; Leites *et al.*, 2012) to field observations of phenotypic trait variation, with the rationale that trees inventoried in the field have a local origin (i.e. seed sources originated within the bioclimatic region inhabited by the trees). In particular, to separate the sources of phenotypic variation in nature, we examined climatic variations that occur at two temporal and spatial scales: first, regional patterns in long-term climate (LTC) that have promoted trait variation among provenances as a result of local adaptation (Savolainen *et al.*, 2007; Mimura & Aitken, 2010; Kremer *et al.*, 2012) – analysed in common gardens by growing different provenances in a same location – and, second, short-term climate (STC) that shapes plastic responses of individual trees to recent climate change (Nicotra *et al.*, 2010; Valladares *et al.*, 2014) – analysed in common gardens by growing the same provenance in different locations. Our approach opens new perspectives for the understanding of phenotypic variation patterns across species distribution ranges using large field observation datasets such as forest inventories.

METHODS

We analysed tree height (m), a fitness-related phenotypic trait, measured both in NFI and common gardens. We selected two major European forest species with contrasted life history traits and ecological requirements: *Abies alba* Mill. (a montane evergreen needle-leaved gymnosperm) and *Quercus petraea* (Matt.) Liebl. (a temperate deciduous broadleaved angiosperm). In the NFI, these two species are traditionally managed using natural regeneration, thus adult trees are assumed to derive from the local gene pool.

We calibrated two independent mixed-effect models of individual tree height using NFI (*in-situ* model) and common garden data (*ex-situ* model), respectively. To validate our models we used two different methods (Fig. 1). The first one is a validation using common garden data: it directly compares the results of the *in-situ* model with independent tree height measurements standardized by common garden and by provenance to respectively separate the effects of the provenance and plasticity. The second one is a validation using *ex-situ* model predictions: it compares the predictions of *in situ* and *ex-situ* models regarding the relative contribution to the model of the climate of the planting site (plastic effect) and that of the climate of the origin of the provenances (provenance effect), and the interaction between both. All analyses and computations were carried out in the R software environment (R Core Team, 2013).

Phenotypic data

National Forest Inventories (NFI)

Observation data comprised ten annual campaigns of the French NFI (2005–2014; http://inventaire-forestier.ign.fr), which consists of a regular grid (1 km^2) of temporary forest plots of 707 m^2 each. In this study, we focused on French NFI (Appendix S1, Fig. S1.1) because inventories of neighbouring countries do not provide age data, thereby preventing the effect of age to be accounted for in models. Nevertheless, the distribution of French NFI plots has a good representativeness of the climatic range of the two species (Fig. S2.1). In each NFI plot, we selected trees for which height (in m), diameter at breast height (dbh; in cm) and age (years) data were measured. In particular, tree age was estimated from wood increment cores collected at breast height (1.30 m) for the one or two of the largest dominant trees in the plot. To account for stand density and the local abundance of neighbouring trees on tree height variation among plots, we computed for each NFI plot the sum of the basal area of neighbouring trees larger than 7.5 cm dbh (Kunstler *et al.*, 2016). We removed plots outside the natural distribution range of the species (Fig. S1.1), identified as plantation or if there was any evidence of recent (<5 years) management, for example logging. We assumed that trees in the remaining plots originated from local provenances within the same bioclimatic region. The final dataset consisted of 5376 trees from 3614 plots for *Q. petraea*, and 1304 trees from 904 plots for *A. alba*.

Common gardens

Common garden data were used to independently validate *in-situ* models (NFI calibration). They were established for breeding purposes during 1990–1996 for *Q. petraea* and 1967–1972 for *A. alba*, as follows: (i) seeds were collected from seed sources (hereafter provenances) throughout the natural distribution range of the species (*N* = 141 for *Q. petraea*, *N* = 47 for *A. alba*); (ii) the seeds were sown in a nursery; (iii) seedlings were transplanted to several sites, i.e., common gardens (*N* = 13 for *Q. petraea*, *N* = 6 for *A. alba*; Fig. S1.1), using a randomised block design; and (iv) measurements of tree height were made at several different years. To avoid pseudo-replication, we randomly selected a single measurement year for each tree. Neighbour basal area was assumed to be constant because plantations have a regular spacing design. Tree age at the time of height measurement was considered to be the time since sowing. A detailed description of the *Q. petraea* provenance tests is provided in a previous study (Sáenz-Romero *et al.*, 2017). A description of the *A. alba* provenances studied in common gardens is provided in Appendix S1 (Tables S1-S2).

Climate data

To analyse phenotypic trait response to long-term climate and recent climate change, we used the yearly climate grids (1901–2014) at 30 arc sec resolution (~1 km^2) of the EuMedClim dataset covering Europe and the Mediterranean Basin (Fréjaville & Benito Garzón, 2018). For the present study, the following bioclimatic variables were considered (Fig. S2.1): annual mean temperature, maximum temperature of the warmest month, minimum temperature of the coldest month, annual precipitation, precipitation of the wettest and the driest month, annual potential evapotranspiration, potential evapotranspiration of the warmest and the coldest month and water balance (precipitation minus potential evapotranspiration) of the wettest and the driest month. EuMedClim was computed following an anomaly approach using the fine 30’ resolution of WorldClim climate means (version 1.4, Hijmans *et al.*, 2005) to adjust the coarse spatial 0.5° resolution of yearly climate data from the Climate Research Unit (version ts3.23, Harris *et al.*, 2014). EuMedClim provides inter-annual variation of bioclimatic conditions at high spatial resolution, allowing the analysis of climate at different spatial and temporal scales instead of using climate means over a reference period (e.g. WorldClim).

To fulfil the requirements of our modelling approach based on the different climate scales at which phenotypic plasticity and local adaptation act, we split the climate data into three different sets of data: (i) long-term climate (LTC) that is the average climate value of the 1901–1960 period, and represents the climate driven local adaptation in the past for provenances (for common gardens) or for a common bioclimatic origin (for NFI, assuming that that all trees have a local origin in a given bioclimatic origin – Appendix S2); (ii) short-term climate (STC) represents the plastic response of trees to recent climate and is calculated as the local climate averaged over the 10 years preceding the measurements (NFI and common garden data); iii) recent climate change (RCC), calculated by subtracting LTC from STC to avoid collinearity problems between LTC and STC in NFI.

Models of intra-specific trait variability

Hereafter, we refer to models calibrated using NFI data as *in-situ* models and to models calibrated using common gardens as *ex-situ* models. For a given species, the phenotypic trait T_{ijk} (tree height) of the i^{th} tree individual of the j^{th} bioclimatic region (or provenance) in the k^{th} plot (or common garden) was modelled as follows:

$$\log(T_{ijk}) = \alpha_0 + \alpha_1 LTC_j + \alpha_2 LTC_j^2 + \alpha_3 RCC_{jk} + \alpha_4 RCC_{jk}^2 + \alpha_5 LTC_j \times RCC_{jk} + \beta + \delta + \varepsilon \qquad (1)$$

where LTC_j is the long-term climate of either the j^{th} bioclimatic region in NFI or the j^{th} provenance in common gardens; RCC_{jk} is the recent climate change defined as the difference between the STC at the k^{th} site (i.e., the NFI plot or the common garden) and LTC_j. We included quadratic terms for both LTC_j and RCC_{jk} to consider non-linear shapes in height responses to climate across species ranges. β includes ontogeny and neighbour basal area covariates and is defined as:

$$\beta = \alpha_6 \log(age_{ijk}) + \alpha_7 \log(BAc_{ijk}) + \alpha_6 \log(age_{ijk}) \times RCC_{jk} + \alpha_7 \log(BAc_{ijk}) \times LTC_j \quad (2)$$

where *age* is the tree age (in years, estimated at breast height in NFI and as the time since sowing in common gardens) and *BAc* is the sum of the basal area of neighbouring trees (assumed to be constant in common gardens). δ gathers random effects and ε is the model error. To control for differences among sampling units in soil fertility, management (or disturbances) and environmental factors not accounted for by fixed effects, we set as random effects the plot nested within the bioclimatic region in *in-situ* models and the block nested within the site in *ex-situ* models (randomised block design). In the case of *A. alba*, the bioclimatic region random effect was not retained because it inflated p-values of LTC terms in the *in-situ* model (high redundancy). One main difference between NFI and common garden data is the age of trees (Fig. S4.1). We reduced this difference by excluding old trees (> 200 years) in NFI and saplings (< 10 years) in common gardens, and we added *age* as a covariate in the models to control for ontogeny. To control for potential differences in growth response to climate change among ontogenic stages, we added the interaction term $age_{ijk} \times RCC_{jk}$ in both models. We also introduced *BAc* as covariate to control for neighbour basal area (Fig. S4.1) and the interaction term $BAc_{ijk} \times LTC_j$ to control for potential differences in neighbour basal area effects among bioclimatic regions in *in-situ* models. A saturated model form including $BAc_{ijk} \times RCC_{jk}$ and $age_{ijk} \times LTC_j$ interaction terms was not retained as they were not significant and decreased model parsimony and the significance of parameters of interest. Models were fitted using the R package nlme (Pinheiro *et al.*, 2015). Coefficients of determination were used to compute the percentage of explained variance by fixed effects alone ($R^2_{marginal}$) and both fixed and random effects ($R^2_{conditional}$) (Nakagawa & Schielzeth, 2013).

For each species, we selected one single explanatory bioclimatic variable to represent LTC and RCC, the same between the two datasets (to enable comparison). The variable selection process was as follows. First, we fitted one model per dataset for each bioclimatic variable (Fig. S2.1) using eqns (1-2). Second, we removed models when parameter estimates for LTC and RCC were not significant at $P = 0.1$ or when positive quadratic relationships were fit ($\alpha_2 > 0$ or $\alpha_4 > 0$) to keep models with decreasing tree height towards one or both ends of the climatic gradient. Third, competitive models were compared using the Akaike information criterion (AIC), and the final model selection was based on the lowest AIC values for both *in-situ* and *ex-situ* models (to enable comparison).

Model predictions

Separating provenance effect, plasticity and their interaction

Model coefficients were used to separate components of phenotypic variation by substituting RCC to its climatic components ($RCC_{jk} = STC_k - LTC_j$) in eqn. (1):

$$\log(T_{ijk}) = \alpha_0 + (\alpha_1 - \alpha_3)\,LTC_j + (\alpha_2 + \alpha_4 - \alpha_5)\,LTC_j^2 + \alpha_3\,STC_k + \alpha_4\,STC_k^2$$

$$+ (\alpha_5 - 2\alpha_4)\,LTC_j \times RCC_{jk} + \beta + \delta + \varepsilon \quad (3)$$

This analytical decomposition enables to estimate the relative effects of the long-term and short-term climate in the field, using RCC and LTC from eqn. (1). From eqn. (3), coefficients associated to linear ($\alpha_1 - \alpha_3$) and quadratic ($\alpha_2 + \alpha_4 - \alpha_5$) variation of LTC are used to predict the effect of the provenance, coefficients associated to linear (α_3) and quadratic (α_4) variation of STC are used to predict phenotypic plasticity (reaction norms) and those associated to $LTC_j \times STC_k$ ($\alpha_5 - 2\alpha_4$) are used to predict their interaction.

Spatial predictions

The *in-situ* and *ex-situ* models were used to make spatial predictions of provenance and plasticity effects, their interaction and the total component of tree height response to climate across Europe. We computed LTC_j and STC_k in each grid cell (30 arc sec resolution) respectively using the long-term (1901–1960) and the recent short-term (2001–2014) averaged values of the corresponding climatic variables to compute maps according to fitted parameters in eqn. (3). Effects of covariates were fixed for *age* (12-year-old trees), *BAc* (30 m^2 ha^{-1}) and for their interaction with RCC_{jk} and LTC_j (both averaged across the species natural range), respectively, according to eqn. (2), and these constants (including the intercept α_0) were added to the total variation component.

Model validation

To validate our approach, we used two alternative methods (Fig. 1) to test the ability of *in-situ* models to predict independent tree height observations in common gardens where the effects of the provenance, plasticity and their interaction can be separated.

Validation using common garden data

To compare the predictions of *in-situ* models with raw common garden data, we first predicted the mean height of each provenance in each site (provenance-by-site mean) from eqn. (3), as a function of the LTC of the provenance and the STC of the site for a given age and neighbour basal area. Then, we compared these predictions to observed values in common gardens. Both predicted and observed provenance-by-site means were standardized across sites and provenances to estimate provenance and plasticity effects, respectively (see

Appendix S3). Correlations between predicted and observed values were tested using Pearson correlation coefficients.

Validation using ex-situ model predictions

To compare the predictions of *in-situ* and *ex-situ* models, we predicted provenance and plasticity effects, and their interaction, as a function of LTC and STC conditions in common gardens using both *in-situ* and *ex-situ* models (see Appendix S3). From eqn. (3), the mean tree height of a provenance planted in several common gardens was predicted for a given age and neighbour basal area as a function of the LTC of the provenance (provenance effect) and the mean tree height of each provenance was predicted as a function of the STC of the site (plasticity of the provenance). Correlations between paired predictions from *in-situ* and *ex-situ* models of provenance and plasticity effects, their interaction and the sum of all three components of tree height (total variation) were tested using Pearson correlation coefficients. For the interaction component, correlation coefficients were computed separately for the mean plastic responses (reaction norms) of cold, core and warm provenances. We classified provenances among cold, core and warm parts of the range using the 1-33th, 34-66th and 67-100th percentiles of LTC, respectively, computed across the natural distribution range of the species.

RESULTS

We found both *in-situ* and *ex-situ* models with significant terms for LTC, RCC and their interaction on individual tree height in *Q. petraea* whereas only the *in-situ* model was found significant for *A. alba*. In *Q. petraea*, selected *in-situ* and *ex-situ* models were based on the maximum temperature of the warmest month (Tmax). In *A. alba*, the selected *in-situ* model was based on the potential evapotranspiration of the warmest month (PETmax). Both *in-situ* and *ex-situ* models indicated significant negative interaction between LTC and RCC (Table 1) and positive interaction between LTC and STC (Table 2) in both species. Hence, average plasticity differed among regions and provenances for both species.

In-situ selected models indicated significant positive effects of tree age and neighbour basal area on tree height (Table 1, Fig. S4.1). Tree height increased with increasing neighbour basal area in *A. alba* (P = 0.07) and with neighbour basal area towards warmer regions in *Q. petraea* (positive interaction between BAc and LTC, P = 0.02; Table 1).

Statistical approximation of provenance and plasticity effects

Sessile oak (Quercus petraea)

Validation using common garden data indicated that predictions of tree height variation among provenances and among sites using the *in-situ* model were significantly correlated with observations in common gardens in *Q. petraea* (P < 0.001 for estimates of provenance and plasticity effects, and the total component of tree height, Fig. S6.3). Validation using *ex-situ* model predictions showed high correlations between *in-situ* and *ex-situ* model predictions of the provenance and plasticity effects, and their interaction (Table 2, Fig. 2). We found significant quadratic responses of height to Tmax for the provenance effect (Fig. 2a), plasticity (Fig. 2b) and the total (Fig. 2c) variation, that were similar between *in-situ* and *ex-situ* models with high correlations between paired predictions (r > 0.80, P < 0.001). We found high correlations between *ex-situ* and *in-situ* model paired predictions of cold (r = 0.65, P < 0.001), core (r = 0.99, P < 0.001) and warm provenance mean reaction norms (r = 0.97, P < 0.001). Both models showed similar patterns in Tmax optimums (i.e. Tmax values corresponding to maximum predicted heights) among cold, core and warm provenances that were respectively warmer and colder for warm and cold provenances (Kruskal-Wallis tests, P

< 0.001, Fig. 2d-e). The *in-situ* model, however, showed higher differences in optimums among provenances (Fig. 2e).

Silver fir (Abies alba)

In *A. alba*, the *in-situ* model showed significant quadratic responses of tree height to PETmax for the provenance and plasticity effects (Table 2). Validation using common garden data indicated that the *in-situ* model significantly predicted tree height variation among provenances in common gardens (provenance effect: $r = 0.44$, $P < 0.01$, Fig. 3a) and among sites (plasticity effect: $r = 0.72$, $P < 0.001$, Fig. 3b). The correlation was weak for the total variation ($r = 0.20$, $P = 0.06$, Fig. 3c, Fig. S7.3). The *in-situ* model predicted warmer optimums for warm provenances and colder optimums for cold provenances (Kruskal-Wallis tests, $P < 0.001$, Fig. 3d).

Range-wide spatial predictions of tree height

In *Q. petraea*, both the *ex-situ* and *in-situ* models predicted very similar spatial patterns (Fig. 4) in the relative variation of tree height for provenance and plasticity effects, and their interaction, despite differences in absolute values for total variation for a given age and neighbour basal area (Fig. 4g-h). These differences are explained by the differences in tree age estimation between the two datasets (i.e. age is measured at breast height in NFI and as the time since sowing in common gardens). The quadratic response of tree height to LTC (Fig. 2a) predicted that trees living at the warm limit of the species range were the shortest, which is illustrated by the short heights predicted over southern Europe from the provenance effect (transparent colours, Fig. 4a-b). Similarly, trees inhabiting the warmest conditions in the southernmost part of the species distribution range were also predicted to be shorter from the phenotypic plasticity effect (Fig. 4c-d). Spatial predictions of interaction effects showed an opposite pattern with increasing height towards warmer climates (Fig. 4e-f). Total variation followed spatial patterns of the provenance and plasticity effects (Fig. 4g-h). In *A. alba*, trees inhabiting cold climates (e.g. high elevation areas in the Alps) were predicted to be shorter according to the *in-situ* model (Fig. 5). In warm climates, the provenance effect (Fig. 4a) and provenance × plasticity interaction (Fig. 5c) predicted taller trees while plasticity predicted smaller trees over southern Europe (Fig. 5b).

DISCUSSION

Can the effects of the provenance and phenotypic plasticity in tree height be inferred from *in-situ* observations?

To date, disentangling the sources of phenotypic variation has only been addressed by analysing common gardens or reciprocal transplant experiments (e.g. Kawecki & Ebert, 2004; Hoffmann & Sgrò, 2011; Blanquart *et al.*, 2013; Latreille & Pichot, 2017), using similar approaches as those that we named here *ex-situ* models. However, as common garden data are often scarce, we propose an alternative method for understanding the causes of phenotypic variation: using increasingly abundant data from field observations, such as NFI. Using the rationale of *ex-situ* models based on common garden data, we defined *in-situ* models based on NFI data and thoroughly validated *in-situ* model predictions with raw data coming from common gardens and with predictions from *ex-situ* models.

Overall, our results show that *in-situ* models correctly predicted phenotypic patterns observed in common gardens (Table 2, Figs 2-5), suggesting that field observations (NFI) can be used to statistically approximate the range-wide intraspecific variation in tree height that is attributable to differences among provenances, plasticity and their interaction. In particular, our results suggest that differences among provenances that are related to their climate of origin can be statistically approximated using field measurements by modelling trait variation as a function of the long-term regional climate (LTC), while the recent climate change (RCC) and its components (STC - LTC) can be used to estimate the plastic response of the trait.

In both species, the most parsimonious models (both *in-situ* and *ex-situ*) were based on climatic variables related to summer temperature: PETmax in *A. alba* and Tmax in *Q. petraea.* This underlies the high sensitivity of *Abies alba* to the evaporative demand in summer (Lebourgeois *et al.*, 2013) and that temperature chiefly drove differences in tree height among *Q. petraea* provenances while drought mostly drove plastic responses for tree height and survival in this species (Sáenz-Romero *et al.*, 2017).

Common patterns of among-provenance variation in tree height plasticity: implications for species distribution ranges under climate change

In both species, we found hump-shaped relationships between height and climate for the provenance (long-term climate) and plasticity effects (short-term climate) and a positive interaction effect between them (Table 2, Figs 2-3). The latter indicated that climatic optima of provenances co-vary positively with their climate of origin: warmer provenances grow taller in warmer climates and colder provenances grow taller in colder climates (Figs 2d-e and 3d), suggesting local adaptation in both species and that plasticity differs significantly among populations (Wang *et al.*, 2006; Leites *et al.*, 2012; Münzbergová *et al.*, 2017; Sáenz-Romero *et al.*, 2017). This consistency between *A. alba* (a mountain evergreen conifer tree) and *Q. petraea* (a temperate deciduous broadleaved tree) points to potential common patterns in local adaptation and plasticity among tree species, as recently indicated in boreal conifer trees (Pedlar & McKenney, 2017).

Our spatial predictions of phenotypic plasticity suggest that tree height of warm provenances has decreased in response to recent climate warming, mostly in southern Europe (Figs 4-5). These results suggest that recent warming may have pushed species at the warmest boundary of the distribution range beyond their tolerance limits, that is corroborated by a higher mortality in warmest/driest range margins for *A. alba*, *Q. petraea* and other European tree species (Cailleret *et al.*, 2014; Benito Garzón *et al.*, 2018). Furthermore, we found that the effect of neighbour basal area on tree height was dependent on the climate of the bioclimatic region in *Q. petraea*, emphasising that tree sensitivity to biotic interaction (e.g. competition) may change along climatic gradients (Gomez-Aparicio *et al.*, 2011; Kunstler *et al.*, 2016).

Limitations and perspectives

Our approach needs an extensive network of common gardens to well identify reaction norms that are at the basis of the models. For instance, in *A. alba* models that are based in significantly less data than those of *Q. petraea*, we did not find any significant *ex-situ* model.

Another limitation of our approach comes from the large difference in the age of trees (older in NFI data) and the fact that NFI data rely on dominant trees, that might partly explained that a stronger signal of local adaptation (i.e. higher differences in climatic optima) was found using NFI data for *Q. petraea* (Fig. 2d).

Finally, the among-provenances differences found by our approach are not only related to local adaptation, but also to neutral, adaptive and even maladaptive components of genetic variation that were not taken into account. New analysis using genomic data across species ranges is the natural next step to fully understand genetic effects (including neutral, adaptive and maladaptive components of genetic variation) in natural and common garden populations (Fitzpatrick & Keller, 2015; Bay *et al.*, 2018; Josephs *et al.*, 2019).

CONCLUSION

We show that phenotypic plasticity, provenance effects and their interaction can be statistically approximated using field observations of wild tree populations subject to recent climate warming. However, further studies are needed to determine whether the ability of *in-situ* models to predict trends in common garden experiments represent a shared underlying cause that can be generalized to other situations, i.e. whether climate variations at different scales can be used to separate local adaptation and plastic responses to climate in field conditions. The modelling framework used in our study could be applied to many species and traits, offering a promising avenue to enhance our understanding of local adaptation and plasticity patterns across large geographical gradients.

REFERENCES

Alberto, F.J., Aitken, S.N., Alía, R., González-Martínez, S.C., Hänninen, H., Kremer, A., Lefèvre, F., Lenormand, T., Yeaman, S., Whetten, R. & Savolainen, O. (2013) Potential for evolutionary responses to climate change – evidence from tree populations. *Global Change Biology*, **19**, 1645–1661.

Bay, R.A., Harrigan, R.J., Underwood, V.L., Gibbs, H.L., Smith, T.B. & Ruegg, K. (2018) Genomic signals of selection predict climate-driven population declines in a migratory bird. *Science*, **359**, 83–86.

Benito Garzón, M., Alía, R., Robson, T.M. & Zavala, M.A. (2011) Intra-specific variability and plasticity influence potential tree species distributions under climate change. *Global Ecology and Biogeography*, **20**, 766–778.

Benito Garzón, M., González-Muñoz, N., Wigneron, J.-P., Moisy, C., Fernández-Manjarrés, J. & Delzon, S. (2018) The legacy of water deficit on populations having experienced negative hydraulic safety margin. *Global Ecology and Biogeography*, **27**, 346–356.

Benito Garzón, M., Robson, T.M. & Hampe, A. (2019) ΔTraitSDM: species distribution models that account for local adaptation and phenotypic plasticity. *New Phytologist*, https://doi.org/10.1111/nph.15716.

Blanquart, F., Kaltz, O., Nuismer, S.L. & Gandon, S. (2013) A practical guide to measuring local adaptation. *Ecology Letters*, **16**, 1195–1205.

Cailleret, M., Nourtier, M., Amm, A., Durand-Gillmann, M. & Davi, H. (2014) Drought-induced decline and mortality of silver fir differ among three sites in Southern France. *Annals of Forest Science*, **71**, 643–657.

Chevin, L.-M., Lande, R. & Mace, G.M. (2010) Adaptation, Plasticity, and Extinction in a Changing Environment: Towards a Predictive Theory. *PLOS Biology*, **8**, e1000357.

Diaz, S., Hodgson, J.G., Thompson, K., Cabido, M., Cornelissen, J.H.C., Jalili, A., Montserrat-Marti, G., Grime, J.P., Zarrinkamar, F., Asri, Y. & others (2004) The plant traits that drive ecosystems: evidence from three continents. *Journal of vegetation science*, **15**, 295–304.

Díaz, S., Kattge, J., Cornelissen, J.H.C., Wright, I.J., Lavorel, S., Dray, S., Reu, B., Kleyer, M., Wirth, C., Colin Prentice, I., Garnier, E., Bönisch, G., Westoby, M., Poorter, H., Reich, P.B., Moles, A.T., Dickie, J., Gillison, A.N., Zanne, A.E., Chave, J., Joseph Wright, S., Sheremet’ev, S.N., Jactel, H., Baraloto, C., Cerabolini, B., Pierce, S., Shipley, B., Kirkup, D., Casanoves, F., Joswig, J.S., Günther, A., Falczuk, V., Rüger, N., Mahecha, M.D. & Gorné, L.D. (2016) The global spectrum of plant form and function. *Nature*, **529**, 167–171.

Duputié, A., Rutschmann, A., Ronce, O. & Chuine, I. (2015) Phenological plasticity will not help all species adapt to climate change. *Global Change Biology*, **21**, 3062–3073.

Fady, B., Cottrell, J., Ackzell, L., Alía, R., Muys, B., Prada, A. & González-Martínez, S.C. (2016) Forests and global change: what can genetics contribute to the major forest management and policy challenges of the twenty-first century? *Regional Environmental Change*, **16**, 927–939.

Fitzpatrick, M.C. & Keller, S.R. (2015) Ecological genomics meets community-level modelling of biodiversity: mapping the genomic landscape of current and future environmental adaptation. *Ecology Letters*, **18**, 1–16.

Frank, A., Howe, G.T., Sperisen, C., Brang, P., St Clair, J.B., Schmatz, D.R. & Heiri, C. (2017) Risk of genetic maladaptation due to climate change in three major European tree species. *Global Change Biology*.

Fréjaville, T. & Benito Garzón, M. (2018) The EuMedClim Database: Yearly Climate Data (1901–2014) of 1 km Resolution Grids for Europe and the Mediterranean Basin. *Frontiers in Ecology and Evolution*, **6**.

Gomez-Aparicio, L., Garcia-Valdes, R., Ruiz-Benito, P. & Zavala, M.A. (2011) Disentangling the relative importance of climate, size and competition on tree growth in Iberian forests: Implications for forest management under global change. *Global Change Biology*, **17**, 2400–2414.

Harris, I., Jones, P. d., Osborn, T. j. & Lister, D. h. (2014) Updated high-resolution grids of monthly climatic observations – the CRU TS3.10 Dataset. *International Journal of Climatology*, **34**, 623–642.

Hijmans, R.J., Cameron, S.E., Parra, J.L., Jones, P.G. & Jarvis, A. (2005) Very high resolution interpolated climate surfaces for global land areas. *International journal of climatology*, **25**, 1965–1978.

Hoffmann, A.A. & Sgrò, C.M. (2011) Climate change and evolutionary adaptation. *Nature*, **470**, 479–485.

Josephs, E.B., Berg, J.J., Ross-Ibarra, J. & Coop, G. (2019) Detecting adaptive differentiation in structured populations with genomic data and common gardens. *Genetics*, https://doi.org/10.1534/genetics.118.301786.

Kawecki, T.J. & Ebert, D. (2004) Conceptual issues in local adaptation. *Ecology letters*, **7**, 1225–1241.

Kremer, A., Ronce, O., Robledo-Arnuncio, J.J., Guillaume, F., Bohrer, G., Nathan, R., Bridle, J.R., Gomulkiewicz, R., Klein, E.K., Ritland, K., Kuparinen, A., Gerber, S. & Schueler, S. (2012) Long-distance gene flow and adaptation of forest trees to rapid climate change. *Ecology Letters*, **15**, 378–392.

Kunstler, G., Falster, D., Coomes, D.A., Hui, F., Kooyman, R.M., Laughlin, D.C., Poorter, L., Vanderwel, M., Vieilledent, G., Wright, S.J. & others (2016) Plant functional traits have globally consistent effects on competition. *Nature*, **529**, 204–207.

Latreille, A.C. & Pichot, C. (2017) Local-scale diversity and adaptation along elevational gradients assessed by reciprocal transplant experiments: lack of local adaptation in silver fir populations. *Annals of Forest Science*, **74**, 77.

Lebourgeois, F., Gomez, N., Pinto, P. & Mérian, P. (2013) Mixed stands reduce Abies alba tree-ring sensitivity to summer drought in the Vosges mountains, western Europe. *Forest Ecology and management*, **303**, 61–71.

Leimu, R. & Fischer, M. (2008) A Meta-Analysis of Local Adaptation in Plants. *PLOS ONE*, **3**, e4010.

Leites, L.P., Robinson, A.P., Rehfeldt, G.E., Marshall, J.D. & Crookston, N.L. (2012) Height-growth response to climatic changes differs among populations of Douglas-fir: a novel analysis of historic data. *Ecological Applications*, **22**, 154–165.

Matyas, C. (1994) Modeling climate change effects with provenance test data. *Tree Physiology*, **14**, 797–804.

Mimura, M. & Aitken, S.N. (2010) Local adaptation at the range peripheries of Sitka spruce. *Journal of evolutionary biology*, **23**, 249–258.

Münzbergová, Z., Hadincová, V., Skálová, H. & Vandvik, V. (2017) Genetic differentiation and plasticity interact along temperature and precipitation gradients to determine plant performance under climate change. *Journal of Ecology*, **105**, 1358–1373.

Nakagawa, S. & Schielzeth, H. (2013) A general and simple method for obtaining R2 from generalized linear mixed-effects models. *Methods in Ecology and Evolution*, **4**, 133–142.

Nicotra, A.B., Atkin, O.K., Bonser, S.P., Davidson, A.M., Finnegan, E.J., Mathesius, U., Poot, P., Purugganan, M.D., Richards, C.L., Valladares, F. & van Kleunen, M. (2010) Plant phenotypic plasticity in a changing climate. *Trends in Plant Science*, **15**, 684–692.

Pedlar, J.H. & McKenney, D.W. (2017) Assessing the anticipated growth response of northern conifer populations to a warming climate. *Scientific Reports*, **7**.

Pinheiro, J., Bates, D., DebRoy, S., Sarkar, D. & R Core Team (2015) nlme: Linear and Nonlinear Mixed Effects Models. R package version 3.1–120. *http://CRAN.R-project.org/package=nlme*.

R Core Team (2013) *R: A language and environment for statistical computing*, R Foundation for Statistical Computing, Vienna, Austria.

Ratcliffe, S., Liebergesell, M., Ruiz-Benito, P., Madrigal Gonzalez, J., Muñoz Castañeda, J.M., Kändler, G., Lehtonen, A., Dahlgren, J., Kattge, J., Peñuelas, J. & others (2016) Modes of functional biodiversity control on tree productivity across the European continent. *Global ecology and biogeography*, **25**, 251–262.

Rehfeldt, G.E., Tchebakova, N.M., Parfenova, Y.I., Wykoff, W.R., Kuzmina, N.A. & Milyutin, L.I. (2002) Intraspecific responses to climate in Pinus sylvestris. *Global Change Biology*, **8**, 912–929.

Ruiz-Benito, P., Ratcliffe, S., Zavala, M.A., Martínez-Vilalta, J., Vilà-Cabrera, A., Lloret, F., Madrigal-González, J., Wirth, C., Greenwood, S., Kändler, G., Lehtonen, A., Kattge, J., Dahlgren, J. & Jump, A.S. (2017) Climate- and successional-related changes in functional composition of European forests are strongly driven by tree mortality. *Global Change Biology*, **23**, 4162–4176.

Sáenz-Romero, C., Lamy, J.-B., Ducousso, A., Musch, B., Ehrenmann, F., Delzon, S., Cavers, S., Chałupka, W., Dağdaş, S., Hansen, J.K., Lee, S.J., Liesebach, M., Rau, H.-M., Psomas, A., Schneck, V., Steiner, W., Zimmermann, N.E. & Kremer, A. (2017) Adaptive and plastic responses of Quercus petraea populations to climate across Europe. *Global Change Biology*, **23**, 2831–2847.

Savolainen, O., Lascoux, M. & Merilä, J. (2013) Ecological genomics of local adaptation. *Nature Reviews Genetics*, **14**, 807–820.

Savolainen, O., Pyhäjärvi, T. & Knürr, T. (2007) Gene flow and local adaptation in trees. *Annual Review of Ecology, Evolution, and Systematics*, 595–619.

Shipley, B., Vile, D. & Garnier, E. (2006) From plant traits to plant communities: a statistical mechanistic approach to biodiversity. *Science*, **314**, 812–814.

Valladares, F., Matesanz, S., Guilhaumon, F., Araújo, M.B., Balaguer, L., Benito-Garzón, M., Cornwell, W., Gianoli, E., Kleunen, M., Naya, D.E. & others (2014) The effects of phenotypic plasticity and local adaptation on forecasts of species range shifts under climate change. *Ecology letters*, **17**, 1351–1364.
Valladares, F., Sanchez-Gomez, D. & Zavala, M.A. (2006) Quantitative estimation of phenotypic plasticity: bridging the gap between the evolutionary concept and its ecological applications. *Journal of Ecology*, **94**, 1103–1116.
Wang, T., Hamann, A., Yanchuk, A., O'neill, G.A. & Aitken, S.N. (2006) Use of response functions in selecting lodgepole pine populations for future climates. *Global Change Biology*, **12**, 2404–2416.
Yeaman, S., Hodgins, K.A., Lotterhos, K.E., Suren, H., Nadeau, S., Degner, J.C., Nurkowski, K.A., Smets, P., Wang, T., Gray, L.K., Liepe, K.J., Hamann, A., Holliday, J.A., Whitlock, M.C., Rieseberg, L.H. & Aitken, S.N. (2016) Convergent local adaptation to climate in distantly related conifers. *Science*, **353**, 1431–1433.

DATA ACCESSIBILITY

Raw data can be freely accessed online for French National Forest Inventories (http://inventaire-forestier.ign.fr), *Quercus petraea* (https://arachne.pierroton.inra.fr/QuercusPortal/) and *Abies alba* common gardens (online repository, under process). Climate data used for this study are available online (http://gentree.data.inra.fr/climate/). R codes used for data analyses can be obtained from the correspondence author upon request.

BIOSKETCH

The authors' research aims to understand how ecological and evolutionary processes drive the effects of global changes on forests, by merging expertise in ecological modelling, genetics and conservation.

T.F. and M.B.G. conceived and designed the study; T.F. conducted the data analyses; T.F. and M.B.G. wrote the manuscript that was commented and improved by B.F., A.K. and A.D.

TABLES

Table 1 Estimates of *in-situ* and *ex-situ* linear mixed-effect models of individual tree height data (log-transformed). *In-situ* models were fit on 5376 trees (height measurements) in 3617 plots nested in 22 bioclimatic regions (random groups) for *Q. petraea* and on 1304 trees in 904 plots nested in 15 bioclimatic regions for *A. alba*. Bioclimatic regions were added as random effects in *in-situ* model for *Q. petraea* but not for *A. alba*. *Ex-situ* models were fit on 130241 trees (height measurements) from 141 provenances that were planted in 591 blocs nested in 13 sites (random groups) for *Q. petraea* and on 13314 trees from 47 provenances planted in 166 blocs nested in 6 sites for *A. alba*. No significant *ex-situ* models were found in *A. alba*. The climatic variable used to compute LTC and RCC is the maximal temperature of the warmest month in *Quercus petraea* and the potential evapotranspiration of the warmest month in *Abies alba*. The percentage of the variance explained by the models is measured by the marginal (fixed effects, m) and conditional (both fixed and random effects, c) adjusted R^2. 'Df' degree of freedom, 'BAc' sum of basal area of neighbouring competitor trees, 'LTC' long-term climate, 'RCC' recent climate change.

Table 2 Mean bootstrap estimates (± SD) of tree height variation due to provenance and plasticity effects, and their interaction, computed from *in-situ* (NFI) model and *ex-situ* (common garden) model. 'x' and 'x^2' indicate linear and quadratic terms respectively. Significant differences of bootstrapped values (n = 200) to null values were tested using t-tests; all are significant at $P < 0.001$.

Table 1

	in-situ				*ex-situ*			
Quercus petraea	**Estimate (±SE)**	**Df**	**t-value**	***P***	**Estimate (±SE)**	**Df**	**t-value**	***P***
Intercept	-13.40 (4.07)	3589	-3.3	0.001	-12.38 (2.23)	129643	-5.54	<0.001
log(age)	0.311 (0.009)	1758	34.53	<0.001	1.322 (0.008)	129643	167.71	<0.001
log(BAc)	-0.171 (0.133)	1758	-1.29	0.197				
LTC	1.269 (0.354)	19	3.59	0.002	0.903 (0.181)	129643	5	<0.001
LTC^2	-0.028 (0.008)	19	-3.58	0.002	-0.020 (0.004)	129643	-5.55	<0.001
RCC	0.440 (0.118)	3589	3.72	<0.001	0.730 (0.182)	129643	4.01	<0.001
RCC^2	-0.017 (0.003)	3589	-5.22	<0.001	-0.018 (0.004)	129643	-4.95	<0.001
LTC:RCC	-0.018 (0.005)	3589	-4.02	<0.001	-0.031 (0.007)	129643	-4.26	<0.001
log(BAc):LTC	0.013 (0.006)	1758	2.38	0.017				
log(age):RCC	0.009 (0.007)	1758	1.3	0.193	-0.012 (0.003)	129643	-3.63	<0.001
R2 (m/c) (%)	41/91				26/65			
Abies alba	**Estimate (±SE)**	**Df**	**t-value**	***P***				
Intercept	0.732 (0.649)	898	-1.13	0.259				
log(age)	0.319 (0.014)	396	23.57	<0.001				
log(BAc)	0.224 (0.123)	396	1.82	0.069				
LTC	0.024 (0.008)	898	2.95	0.003				
LTC^2	$-7.3\ 10^{-5}$ ($2.8\ 10^{-5}$)	898	-2.63	0.009				
RCC	0.009 (0.006)	898	1.46	0.146				
RCC^2	$-9.9\ 10^{-5}$ ($2.3\ 10^{-5}$)	898	-4.36	<0.001				
LTC:RCC	$-8.3\ 10^{-5}$ ($3.8\ 10^{-5}$)	898	-2.17	0.030				
log(BAc):LTC	$-2.4\ 10^{-4}$ ($9.5\ 10^{-4}$)	396	-0.25	0.803				
log(age):RCC	0.002 ($8.4\ 10^{-4}$)	396	1.92	0.056				
R2 (m/c) (%)	49/86							

Table 2

	Provenance effect		Phenotypic plasticity		interaction
	x	**x^2**	**x**	**x^2**	
Quercus petraea	0.191	$-7.3\ 10^{-3}$	0.712	-0.017	$4.6\ 10^{-3}$
***ex-situ* model**	(0.026)	$(0.35\ 10^{-3})$	(0.169)	(0.003)	$(0.68\ 10^{-3})$
Quercus petraea	0.548	-0.022	0.465	-0.018	0.018
***in-situ* model**	(0.365)	(0.009)	(0.122)	(0.003)	(0.007)
Abies alba	0.014	$-8.6\ 10^{-5}$	0.010	$-9.2\ 10^{-5}$	$1.0\ 10^{-4}$
***in-situ* model**	(0.007)	$(2.1\ 10^{-5})$	(0.007)	$(2.1\ 10^{-5})$	$(0.4\ 10^{-4})$

FIGURES

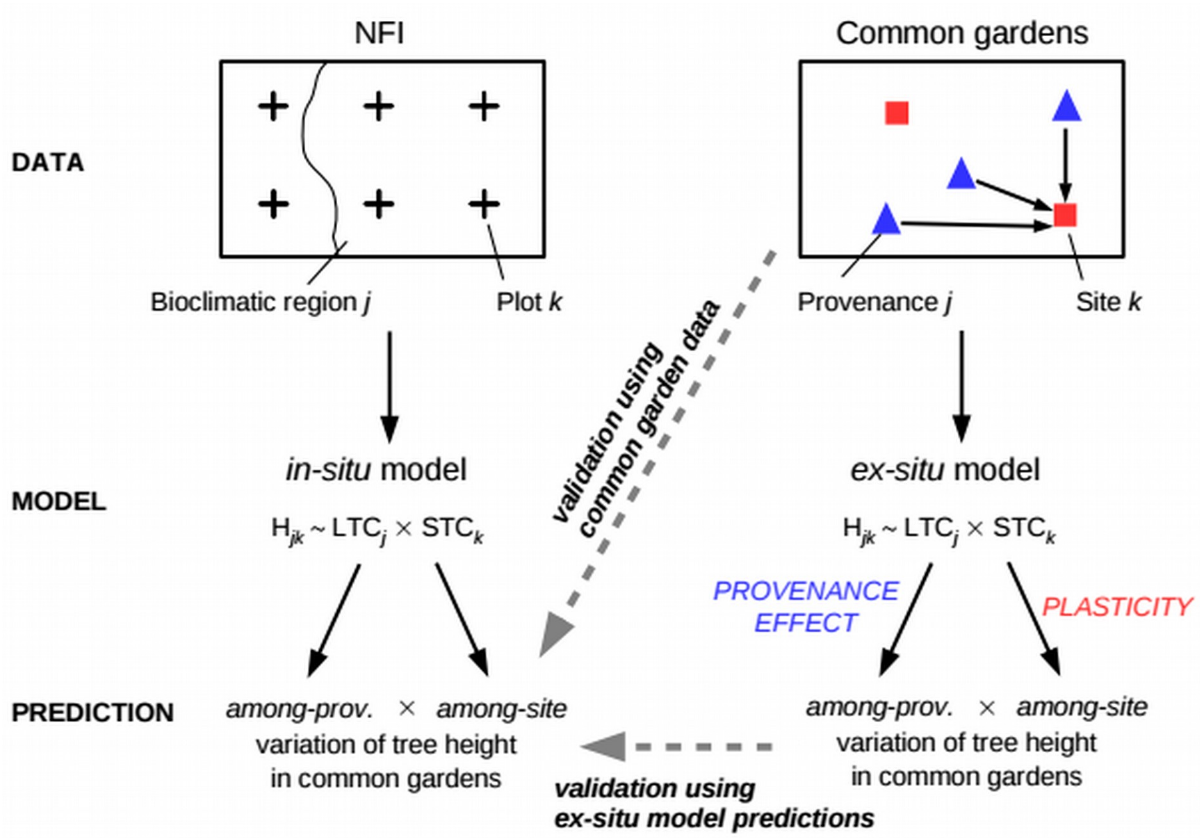

Figure 1 Workflow of the modelling approach and validation methods. We used individual tree height data from National Forest Inventories (NFI) to calibrate a mixed-effect model (‘*in-situ* model’) as a function of long-term climate (LTC) of the bioclimatic region and short-term climate (STC) of the forest plot to disentangle local adaptation, plasticity and their interaction on intraspecific trait variation. To validate our approach, we compared *in-situ* model predictions with independent observations of tree height variation in common gardens where trait differences among populations of different geographical origin (i.e., the provenance) and their plasticity can be separated. *In-situ* model predictions of tree height variation among provenances and among planting sites were compared to observations in common gardens (*validation using common garden data*) and to predictions from a parallel model calibrated using common garden data (*validation using ex-situ model predictions*). *Validation using ex-situ model predictions* needs common garden data covering large climatic gradients (as is the case of *Quercus petraea* in this study) which is not always feasible, while *validation using common garden data* can be used also with scarce common data networks (as is the case of *Abies alba* in this study).

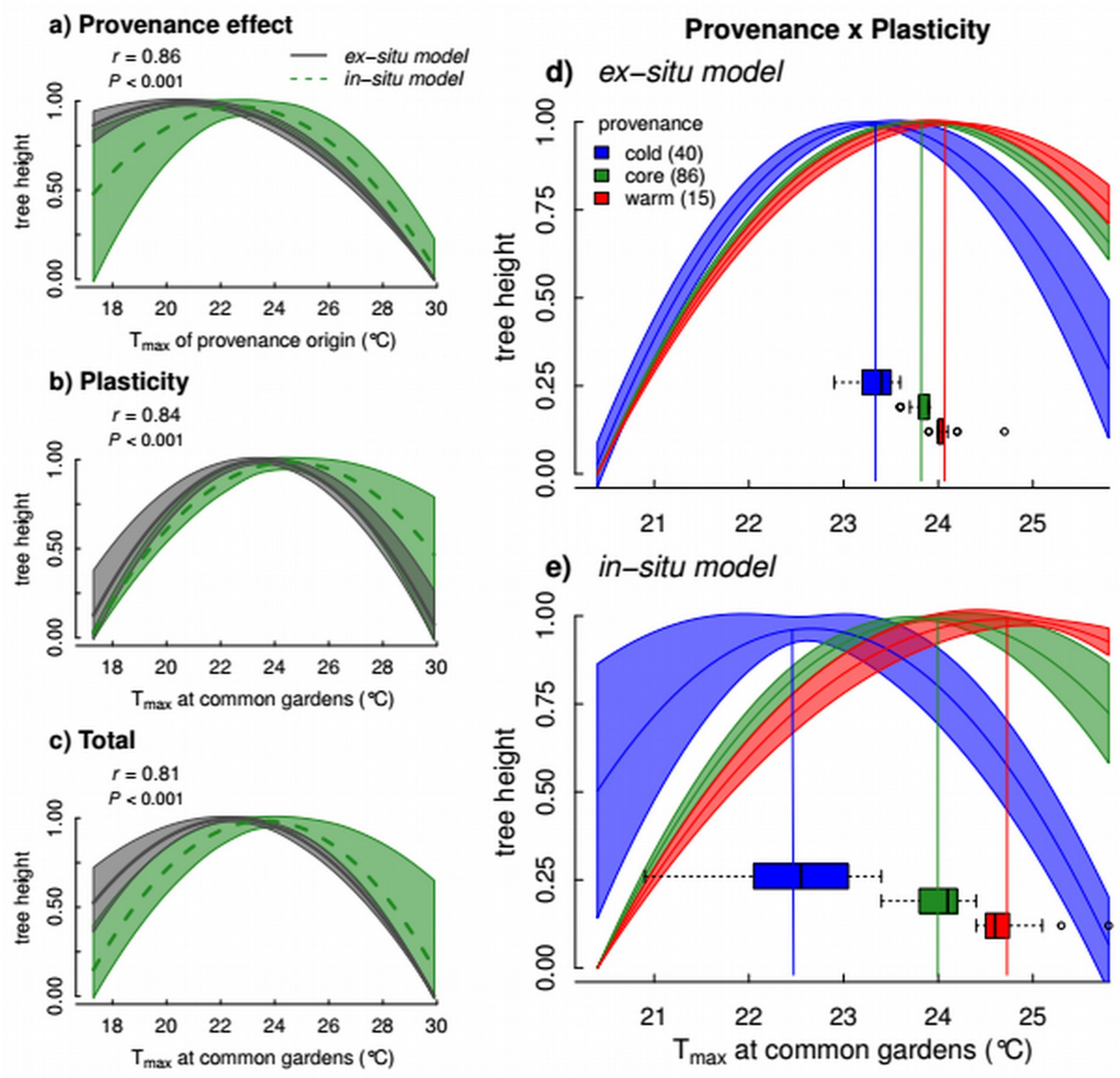

Figure 2 Comparison of *in-situ* model (NFI) and *ex-situ* model (common gardens) predictions of provenance (a) and plasticity effects (b), and the total component (c) of tree height variation, recorded in common gardens in *Quercus petraea*. Pearson correlation coefficients between *ex-situ* and *in-situ* model predictions are reported. (d-e) Model predictions of plastic responses among provenances (provenance × plasticity interaction). Temperature optima for cold, core and warm provenances are indicated by horizontal boxplots; vertical coloured lines indicate mean optimum values. Significant differences in temperature optimum were tested using Kruskal-Wallis tests: $\chi^2 = 105.2$ in d) and $\chi^2 = 104.2$ in e), $P < 0.001$ for both. Shaded areas and lines represent the standard deviation around average model predictions (computed by bootstrapping in a-c). Predictions were scaled between 0–1 independently for *in-situ* and *ex-situ* models. Model parameters (coefficients and significance) are presented in Table 1. Validation analyses using common garden data are presented in Appendix S3.

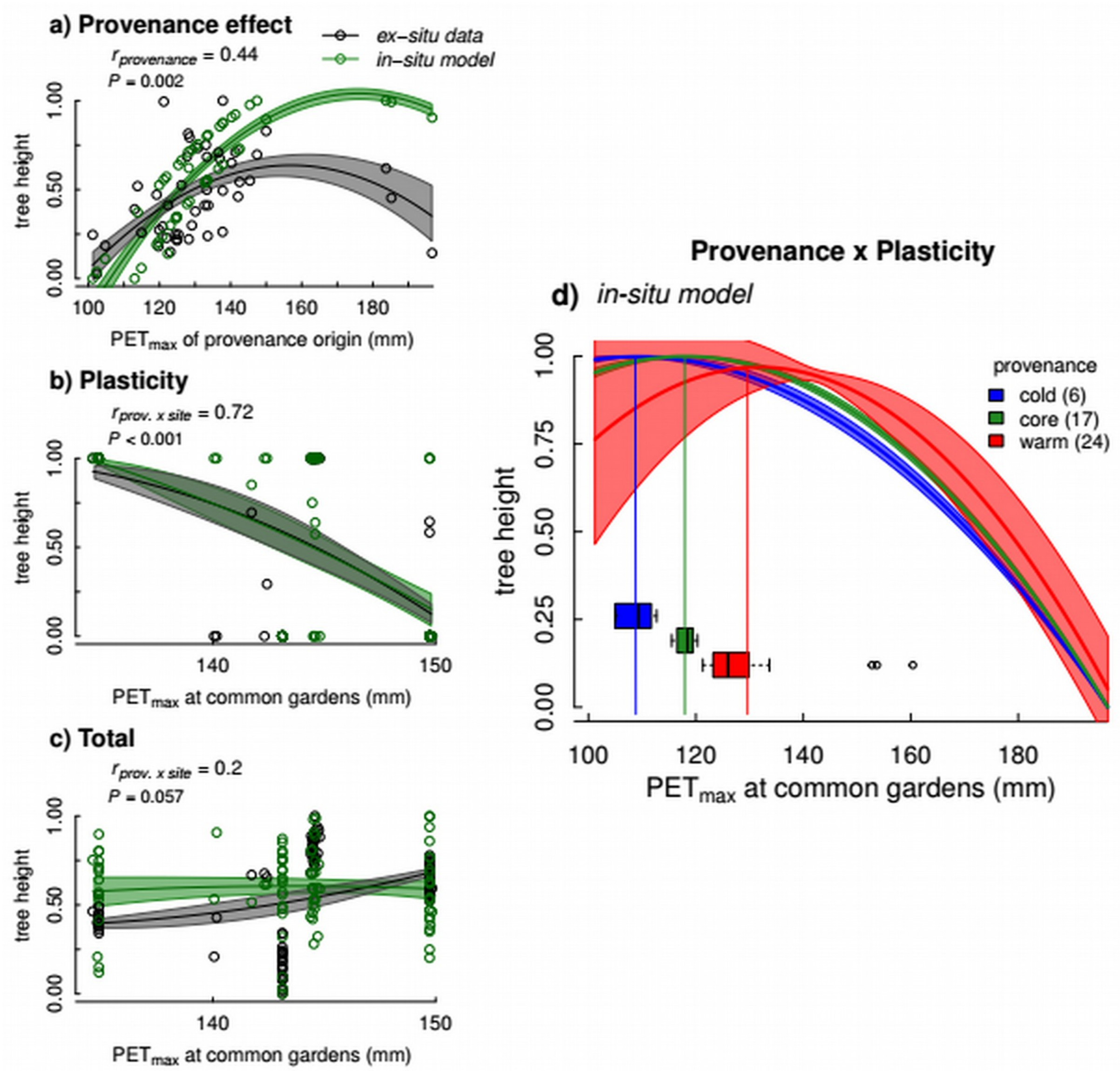

Figure 3 Comparison of *in-situ* (NFI) model predictions and common garden data (*ex-situ*) estimates of provenance (a) and plasticity effects (b), and the total component (c) of tree height variation, recorded in common gardens in *Abies alba*. Points represent provenance means in a) and provenance-by-site means in b-c that were computed according to the validation method using common garden data (see Fig. 1). Computation of provenance and plasticity effects, and the total variation is described in Appendix S3. Pearson correlation coefficients between *ex-situ* data and *in-situ* model predictions are reported. (d) *In-situ* model predictions of plastic responses among provenances (provenance × plasticity interaction). Temperature optima for cold, core and warm provenances are indicated by horizontal boxplots; vertical coloured lines indicate mean optimum values. Significant differences in temperature optimum were tested using Kruskal-Wallis tests: $\chi^2 = 105.2$, $P < 0.001$. Shaded areas and lines represent the standard deviation around average model predictions (computed by bootstrapping in a-c). Height values were scaled between 0–1 independently for *in-situ* predictions and common garden data. *In-situ* model parameters (coefficients and significance) are presented in Table 1.

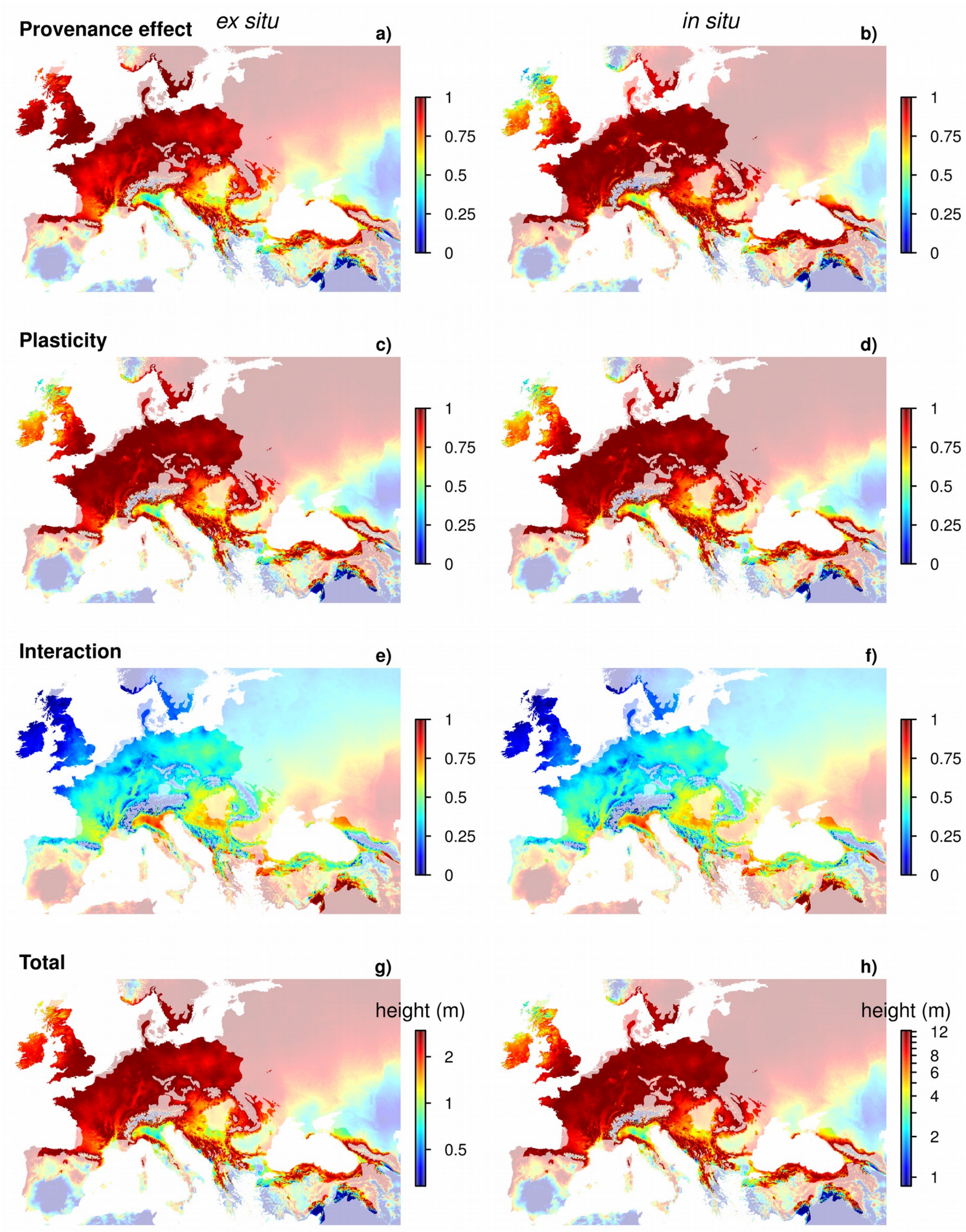

Figure 4 Spatial predictions of *Quercus petraea* range-wide variation in tree height using *ex-situ* (a, c, e, g) and *in-situ* models (b, d, f, h). Maps indicate the provenance effect (a-b), plasticity (c-d), their interaction (e-f) and the total variation of tree height (g-h). The shaded area represents model predictions outside the natural distribution range of the species. Predictions are for 12-years-old trees, with neighbour basal area set to average conditions (30 m^2 ha^{-1}) in the *in-situ* model.

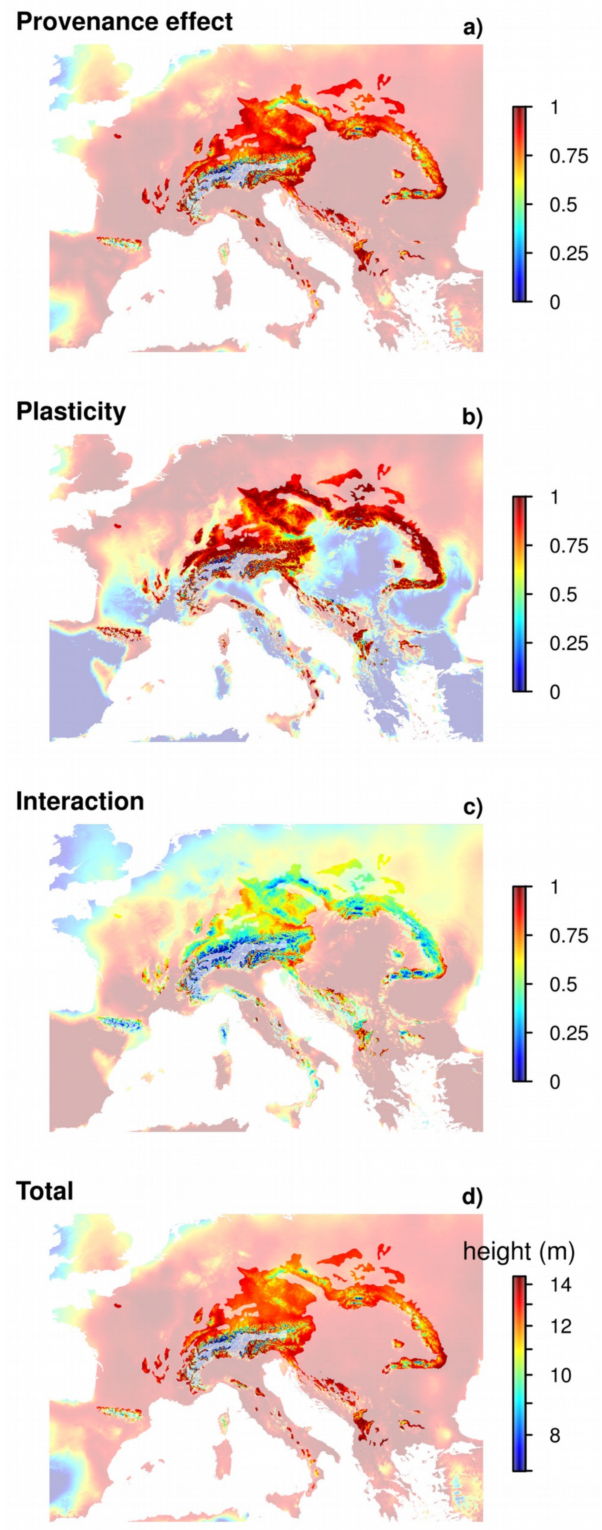

Figure 5 Spatial predictions of *Abies alba* range-wide variation in tree height using the *in-situ* model. Maps indicate the provenance effect (a), plasticity (b), their interaction (c) and the total variation of tree height (d). The shaded area represents model predictions outside the natural distribution range of the species. Predictions are for 12-years-old trees, with neighbour basal area set to average conditions (30 m^2 ha^{-1}).

SUPPORTING INFORMATION

Inferring phenotypic plasticity and population responses to climate across tree species ranges using forest inventory data

Thibaut Fréjaville, Bruno Fady, Antoine Kremer, Alexis Ducousso, Marta Benito-Garzón

Appendix S1 Phenotypic and climate data

Fig. S1.1 Maps of *NFI* and *common garden* tree height data for *Quercus petraea* and *Abies alba*.

Fig. S2.1 Principal component Analysis of climatic conditions across *NFI* and *common garden* data for *Quercus petraea* and *Abies alba*.

Fig. S3.1 Temporal trends (1901–2014) in annual mean temperature across species ranges.

Fig. S4.1 Tree height variation as a function of tree age and neighbour basal area.

Table S1 Description of the 6 common gardens used for measuring tree height on *Abies alba* provenances.

Table S2 Description of *Abies alba* provenances planted in the 6 common gardens.

Appendix S2 Bioclimatic regionalisation of species' natural distribution ranges

Fig. S5.2 Maps of bioclimatic regions within the natural distribution range of *Quercus petraea* and *Abies alba.*

Appendix S3 Model Validation

Validation using common garden data

Fig. S6.3 Correlation between *in-situ* model predictions and common garden data estimates of provenance and plasticity effects and the total component of variation in tree height in *Quercus petraea*.

Fig. S7.3 Correlation between *in-situ* model predictions and common garden data estimates of provenances and plasticity effects and the total component of variation in tree height in *Abies alba*.

Validation using ex-situ model predictions

Appendix S1 Phenotypic and climate data

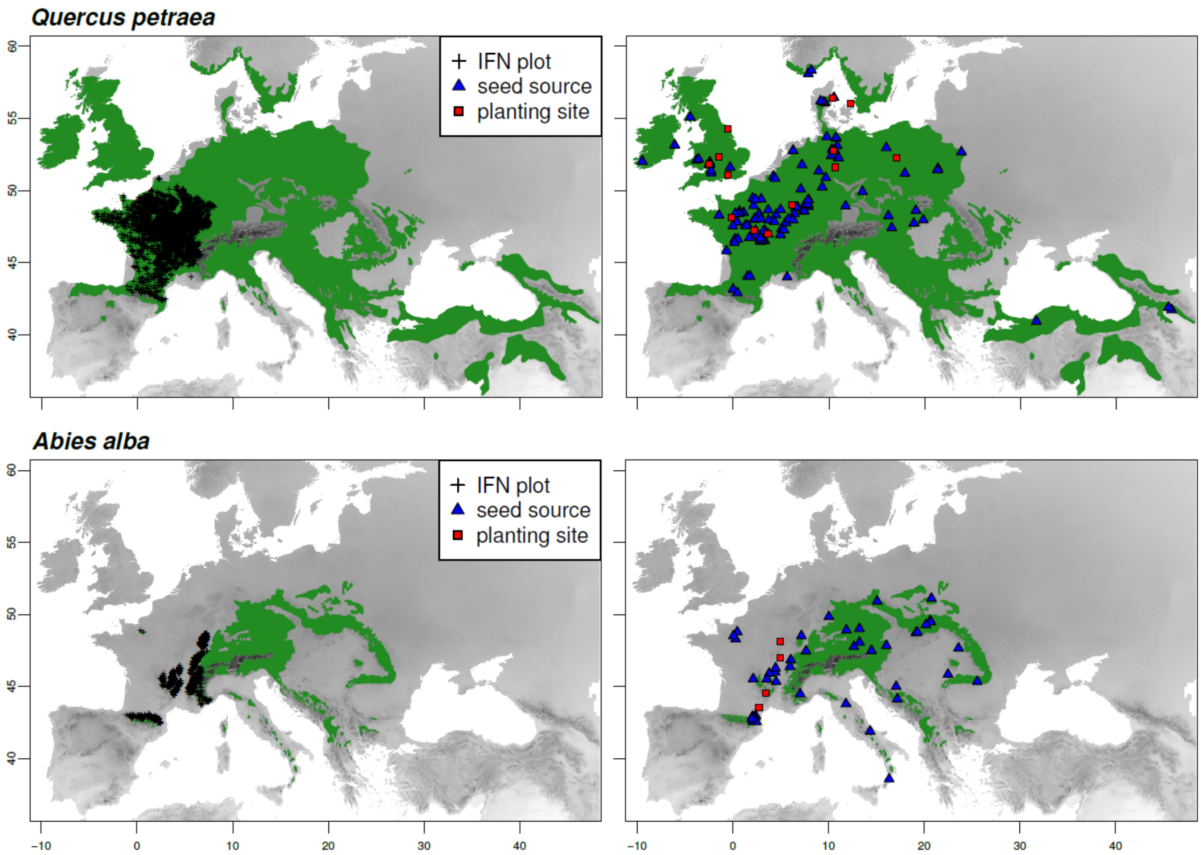

Figure S1.1 Geographic distribution of French National Forest Inventory data (NFI) and common garden experiments within the natural distribution range of *Quercus petraea* and *Abies alba*. Black crosses represent NFI temporary forest plots (left panels) in which height, age and diameter at breast height were measured on dominant trees, within the natural distribution range of the species (green area; http://www.euforgen.org). Common garden experiments (right panels) consist of planted trees from provenances (seed sources, blue triangles) covering the species distribution range in common gardens (genetic trials, red squares).

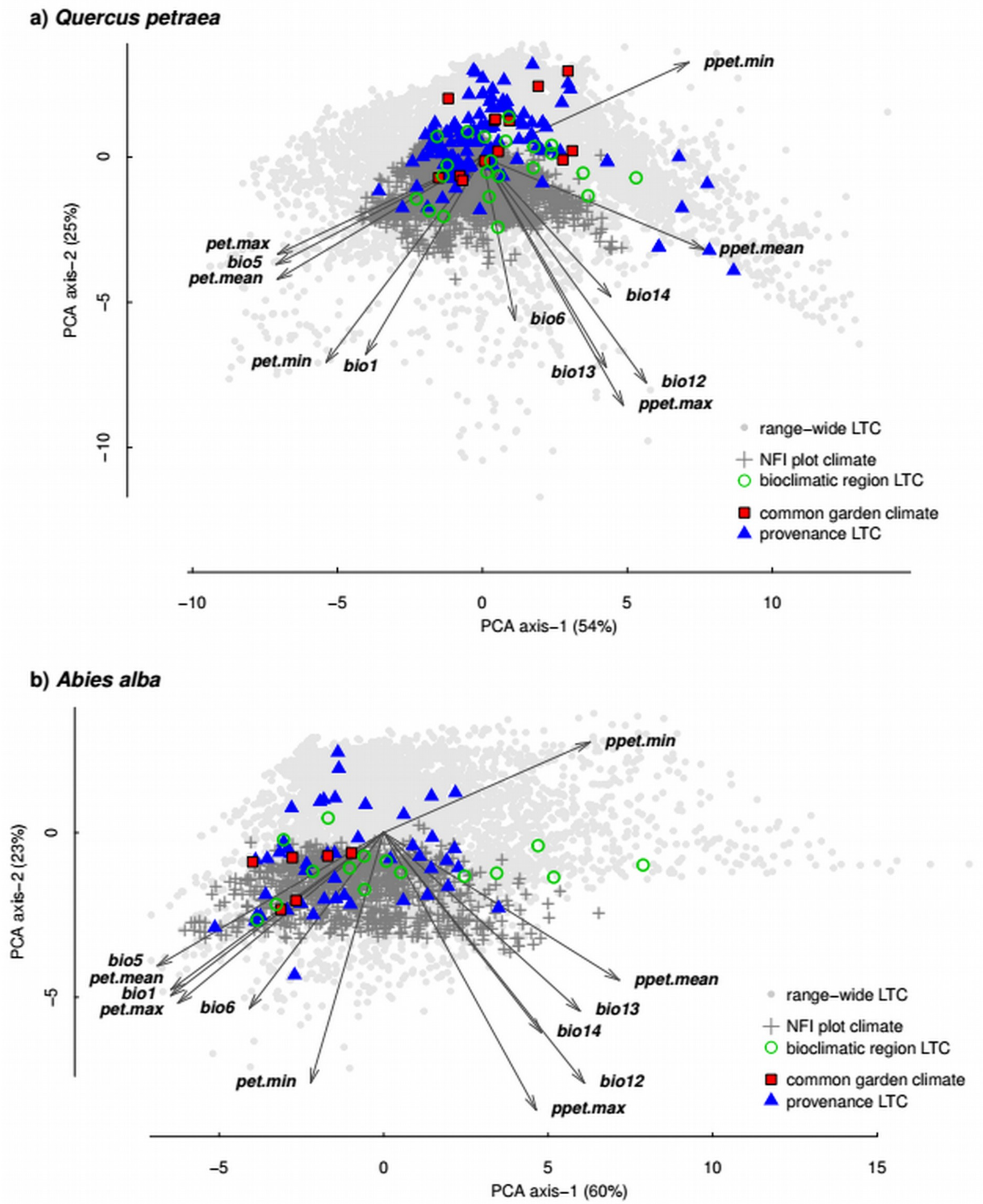

Figure S2.1 Principal component analysis (PCA) of short-term climate at *in-situ* National Forest Inventory (NFI) plots (grey crosses) and *ex-situ* common gardens (red squares), and of long-term climate (LTC) of origin of populations planted in common gardens (‘provenance’, blue triangles) and of bioclimatic regions covered by NFI plots (black circles, see Appendix S2) for *Quercus petraea* (a) and *Abies alba* (b). The LTC distribution across the species natural distribution range is indicated by grey dots. Short-term climate represents the 10-yr means before tree measurements and LTC the 1901–1960 means. The climatic variance explained by the first two PCA axes is indicated in brackets. The PCA was computed using the following climatic variables downscaled from EuMedClim: ‘bio1’ annual mean temperature, ‘bio5’ maximum temperature of the warmest month, ‘bio6’ minimum temperature of the coldest month, ‘bio12’ annual precipitation, ‘bio13’ maximum precipitation of the wettest month, ‘bio14’ minimum precipitation of the driest month, ‘pet.mean’ annual potential evapotranspiration, ‘pet.max’ potential evapotranspiration of the warmest month, ‘pet.min’ potential evapotranspiration of the coldest month, ‘ppet.mean’ annual water balance (precipitation minus evapotranspiration), ‘ppet.max’ water balance of the wettest month, ‘ppet.min’ water balance of the driest month.

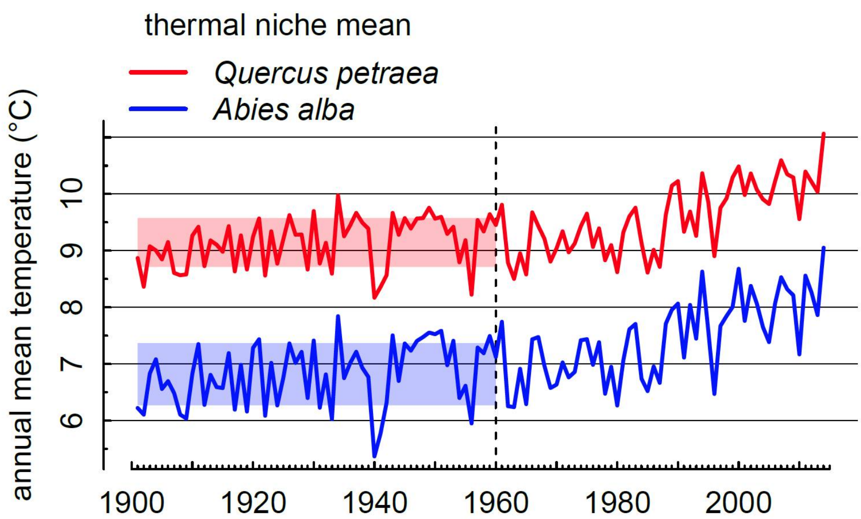

Figure S3.1 Temporal variation (1901–2014) in annual mean temperature (from http://gentree.data.inra.fr/climate/) averaged within the natural distribution range of *Quercus petraea* (red) and *Abies alba* (blue). Shaded area represents the standard deviation around the long-term average climate (1901–1960), prior to the acceleration of climate warming during the decades following 1960. The shapes of species distribution maps used to compute the temporal variation of the thermal niches were sourced from Euforgen (http://www.euforgen.org).

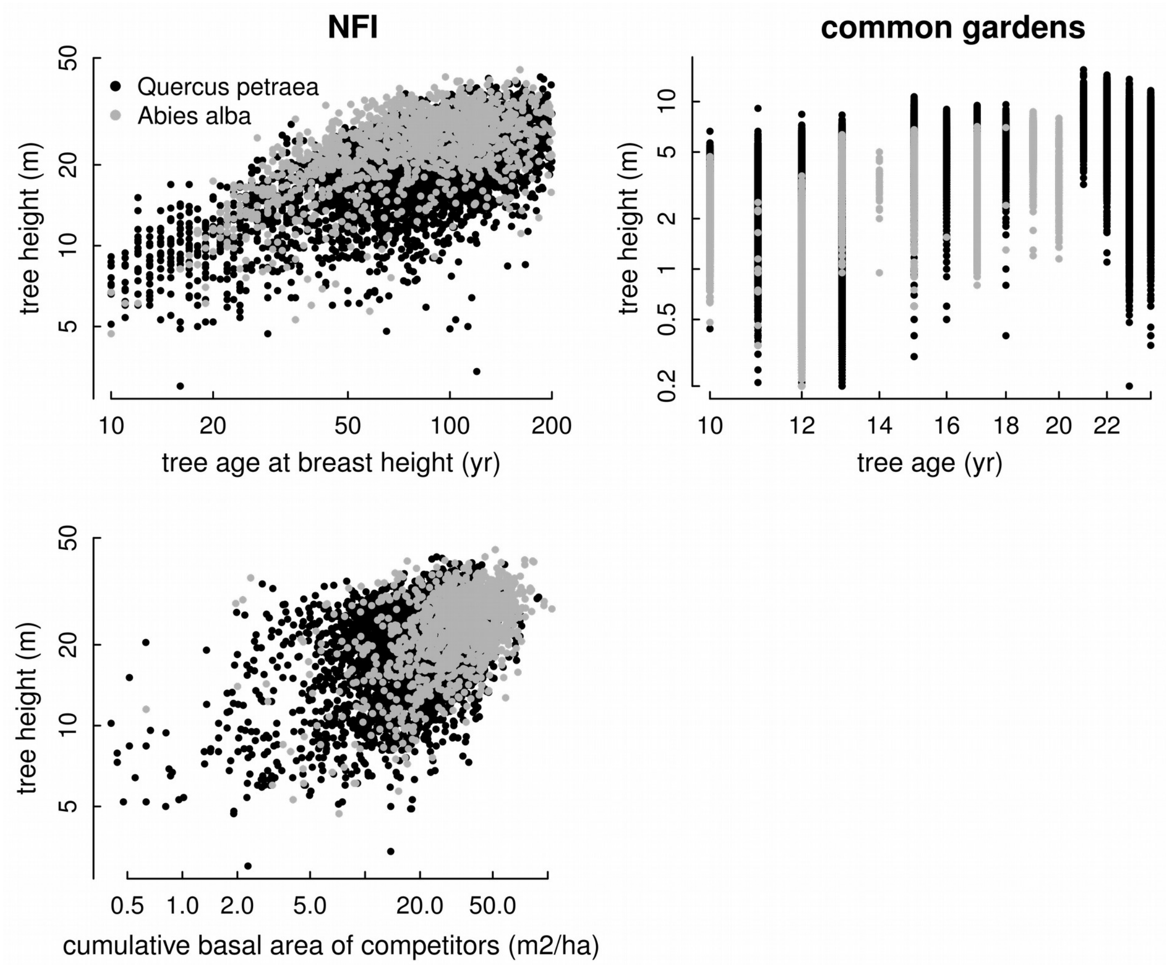

Figure S4.1 Tree height variation as a function of tree age (top) and neighbour basal area (bottom) in *Quercus petraea* (black) and *Abies alba* (grey) in National Forest Inventories (NFI, left) and common gardens (right). Neighbour basal area was assumed to be constant between and within common gardens. Tree age was estimated using wood increment cores collected at breast height (1.30 m) in NFI plots, whereas tree age is the time between the height measurement and the sowing date in common gardens. Note a log scale on both axes.

Table S1 Description of the 6 French common gardens used for measuring phenotypic traits on *Abies alba* provenances. Data include: test site code (as in Table S3), name of forest where the site is located, name of region where the site is located, latitude (in degree decimal, to the 4th decimal point), longitude (in degree decimal to the 4th decimal point), elevation (m a.s.l.), total size of the test site (in hectare), plantation density (trees per hectare) and number of *A. alba* provenances tested in the study (N).

Site code	Site name	Latitude	Longitude	Elevation	Planting date	Size	Density	N
60301	Bois Génard	48.1167	4.9833	320	1972	3	2500	2
70201	Rouvre Sur Aube	47.0167	4.9667	410	1967	3.88	2500	21
70203	La Brugère	44.5667	3.4517	1110	1967	3.22	2000	16
70402	Les Chauvets	44.5667	3.4483	1050	1972	4.31	2500	20
70502	Somail Chinchidou	43.5333	2.7333	920	1973	0.29	10000	35
70503	Somail Sagnassol	43.5361	2.7347	973	1973	0.42	2500	33

Note: the test site may contain other genetic material than the populations tested in this study, e.g. other species irrelevant to this study.

Table S2 Description of *Abies alba* Mill. provenances in the 6 common gardens. Data include: population code number and name, geographic coordinates in degree decimal, country of origin, and number of blocks (replicates) per site where the population is planted. 'B&H' Bosnia & Herzegovina, 'Czech' Czech Republic.

Pop. code	Pop. name	Latitude	Longitude	Country	60301	70201	70203	70402	70502	70503
36549	FORE	45.517	3.550	France		5	5			
36550	GRBO	45.350	4.517	France		5	5			
36555	RUHP	47.767	12.650	Germany					80	32
36556	BEAR	42.967	2.400	France		5	5			
36557	RIAL	42.950	2.367	France		5				
36558	NEBS	42.900	2.133	France		5	5			
36559	PUIV	42.900	2.033	France		6	5			
36560	CALL II	42.850	2.117	France		5	5			
36561	FANG II	42.833	2.283	France		5				
36562	LAFA	42.767	2.000	France		6	5			
36563	BALC	42.583	2.100	France		7	5			
36564	CANG	42.550	2.450	France		6	5			
36565	JOUX II	46.850	6.050	France		5	5			
36566	DONO	48.517	7.167	France		5	5			
36567	BOAJ	46.283	4.467	France		5	5			
36568	MOLL	46.000	4.433	France		5				
36569	BONO II	45.917	3.800	France		5	5			
36570	JASO	45.533	2.133	France		5				
36571	ECOU II	48.517	0.067	France		7	5			
36572	PERS	48.300	0.300	France		5				
36573	LASU	47.667	23.583	Romania		6	5			
36574	PRAH	45.350	25.550	Romania		8	5			
36575	BLIZ	51.117	20.750	Poland					80	32
36576	LA-SU II	45.850	22.483	Romania	5				80	32
36577	KURN	49.850	10.033	Germany					80	32
36578	PRAZ	44.483	7.050	Italy					80	32
36579	KOZA	45.000	17.063	B&H					80	32
36580	FANG IV	42.817	2.267	France				5	80	32
36581	ZWIE	49.017	13.233	Germany					80	32
36582	CALL IV	42.869	2.087	France					80	32
36583	CAMA	43.800	11.817	Italy					80	32
36585	TRIE	47.486	14.486	Austria					80	32
36586	RYTR	49.490	20.668	Poland					80	32
36588	KOBE	48.067	13.233	Austria					80	32
36589	VODC	44.135	17.189	B&H					80	32
36590	KELH	48.917	11.868	Germany					80	32
36591	SEVR II	48.791	0.464	France				6	80	
36592	JOUX III	46.376	5.972	France	5			5	80	32
36594	ROSE	41.900	14.350	Italy					80	32
36596	HOHE	47.834	16.048	Austria					80	32
36597	STSA	49.563	20.636	Poland					80	32
36598	SBRU	38.583	16.333	Italy					80	32
36602	BANS	48.733	19.149	Slovakia					80	32
36603	SLLU	48.767	19.275	Slovakia					80	32
36604	PODS	49.283	20.183	Slovakia					80	32
36606	FRYD	50.921	15.079	Czech					80	32
36607	LOCH	47.457	7.640	Switzerland					80	32

Appendix S2 Bioclimatic regionalisation of species natural distribution ranges

In contrast to the common garden experiments, the geographical origin of the seed source (i.e., the provenance) is unknown for NFI observations. To overcome this major limitation, we made the neutral assumption that the trees have a local origin. In other words, we assume that potential seed sources were mostly from local provenances within the bioclimatic region with a low probability of long-distance transfer. We therefore performed a fine bioclimatic partitioning of the species' natural distribution range (Figure S5.2). The long-term climate of origin (LTC) was estimated as the long-term (1901-1960) average climate of the bioclimatic region in NFI. The recent climate change (RCC) is estimated as the difference between the recent short-term climate (STC) experienced by the tree in the NFI plot (averaged over the last decade of growth before tree height measurement) and the estimated LTC for the corresponding climatic variable.

For each species, the natural distribution range (http://www.euforgen.org) was partitioned into bioclimatic regions by K-means clustering using the R package vegan (Oksanen et al. 2013) (Figure S5.2). We used the Caliński–Harabasz criterion (Caliński & Harabasz 1974) to select a statistically optimal number of regions (K = 70 for A. alba; K = 90 for Q. petraea) from a range of K (10 to 200 in steps of 10). Partitioning of bioclimatic regions was performed on Z-scores (standardised data) of long-term (1901–1960) averages of the following four climatic parameters: minimum temperature of the coldest month (°C), maximum temperature of the warmest month (°C), and total precipitation in the driest and the wettest months (mm); in addition to the latitude and longitude of the plots.

References:

Caliński, T. & Harabasz, J. (1974) A dendrite method for cluster analysis. *Commun. Stat.* 3, 1–27.

Oksanen, J. et al. (2013) vegan: Community Ecology Package. R package version 2.0-7.

Pinheiro, J., Bates, D., DebRoy, S., Sarkar, D. & R Core Team (2015) nlme: Linear and Nonlinear Mixed Effects Models. R package version 3.1–120. HttpCRANR-Proj.

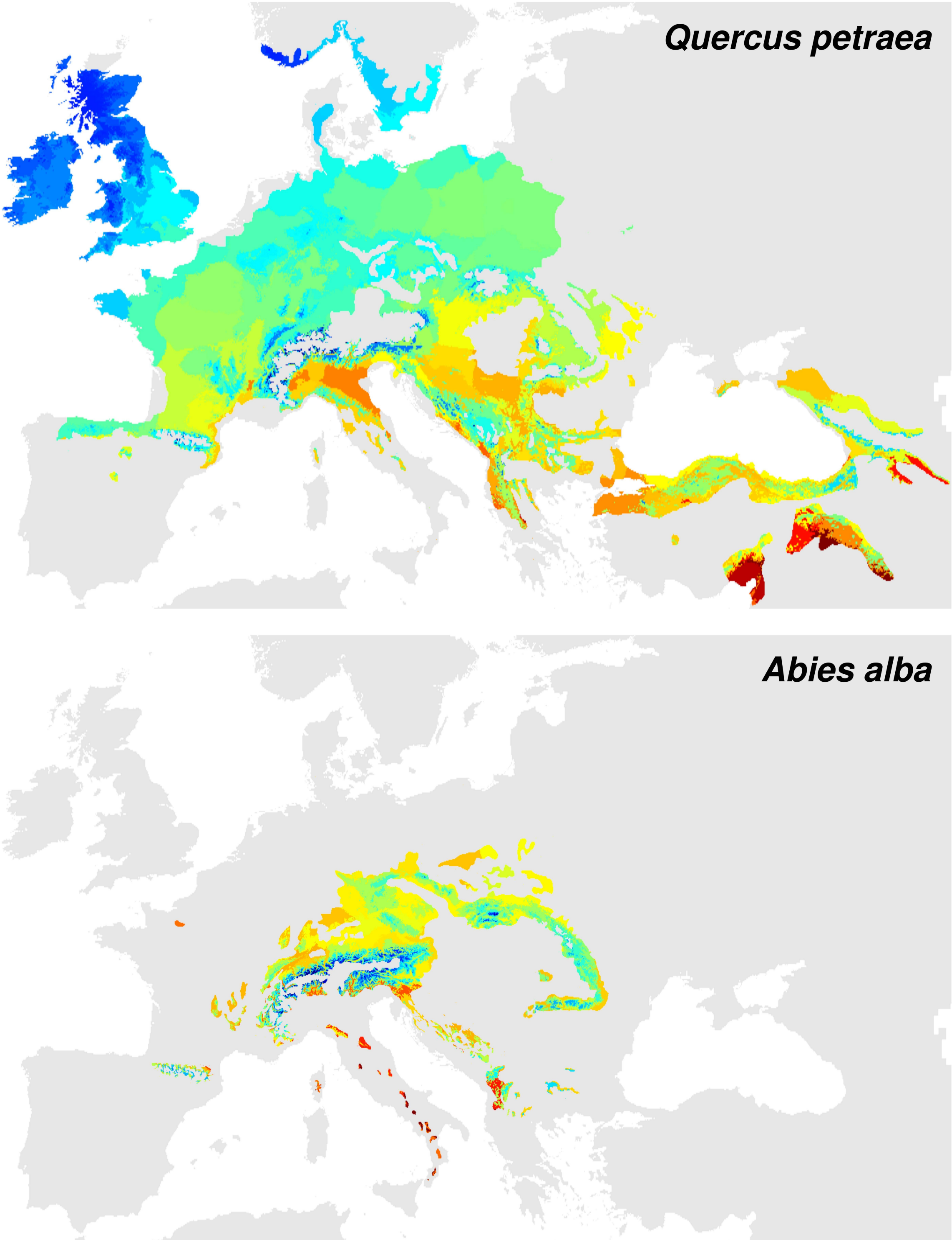

Figure S5.2 Bioclimatic regions within the natural distribution range of *Quercus petraea* (top) and *Abies alba* (bottom). Colour gradient represents differences in long-term regional average (1901–1960) of annual mean temperature, from blue (coldest regions) to red (warmest regions). Discontinuous areas of similar colour indicate a similar long-term mean temperature between bioclimatic regions. Number of bioclimatic regions across species ranges: N = 90 and N = 70 for *Q. petraea* and for *A. alba* respectively.

Appendix S3 Model validation

Validation using common garden data

In the case of validation by comparing the predictions of *in-situ* models with raw common garden data, we standardized both predictions and raw data for differences in provenances, sites, age and neighbour basal area. First, the *in-situ* model was used to predict the mean height of each provenance in each site (‘provenance-by-site’ means) from equation 3 (main text), using the LTC of the provenance and the STC of the site (i.e. common garden) for a given age (12-year-old trees, i.e. the most common age at the time of height measurements across common gardens in both species) and neighbour basal area (30 m^2 ha^{-1}). Second, common garden data were standardized across ages using a linear mixed-effect model, where the log of tree height was regressed against the log of age with the provenance and the site set as random effects. In particular, we used model residuals computed from fixed effects only (i.e. age) to compute provenance-by-site means for common garden observations. Third, provenance-by-site means of common garden observations and *in-situ* model predictions were standardized as follows, before comparing them using Pearson correlation coefficients.

To estimate differences in tree height among provenances (provenance effect), provenance-by-site means were standardized (height values scaled between 0-1) independently for each site. In this way, we focused on height differences among provenances after accounting for differences in environmental conditions among sites (i.e. phenotypic plasticity effect). Then, we computed mean values by provenance. Pearson coefficients indicated significant correlations between common garden data and *in-situ* model predictions for the provenance effect in *Quercus petraea* (Fig. S6.3a) and *Abies alba* (Fig. S7.3a). Moreover, *in-situ* model predictions well predicted tree height differences among cold, core and warm provenances, as indicated by boxplots (Figs S6.3a and S7.3a).

To estimate plasticity, provenance-by-site means were standardized (height values scaled between 0-1) independently for each provenance. In this way, we focused on height differences among sites after accounting for the provenance effect. Pearson coefficients indicated significant correlations between common garden data and *in-situ* model predictions for the plastic component in *Q. petraea* (Fig. S6.3b) and *A. alba* (Fig. S7.3b). Considering cold, core and warm provenances separately, correlations were still significant at $P < 0.05$.

To estimate the total component of variation (sum of provenance effect and provenance plasticity effect), provenance-by-site means were standardized across all data (height values scaled between 0-1). Pearson coefficients indicated weak correlations in both species, significant in *Q. petraea* at $P < 0.001$ (Fig. S6.3c) and in *A. alba* at $P < 0.10$ (Fig. S7.3c). *In-situ* model predictions reasonably predicted height differences among cold, core and warm provenances, as indicated by boxplots (Figs S6.3c and S7.3c).

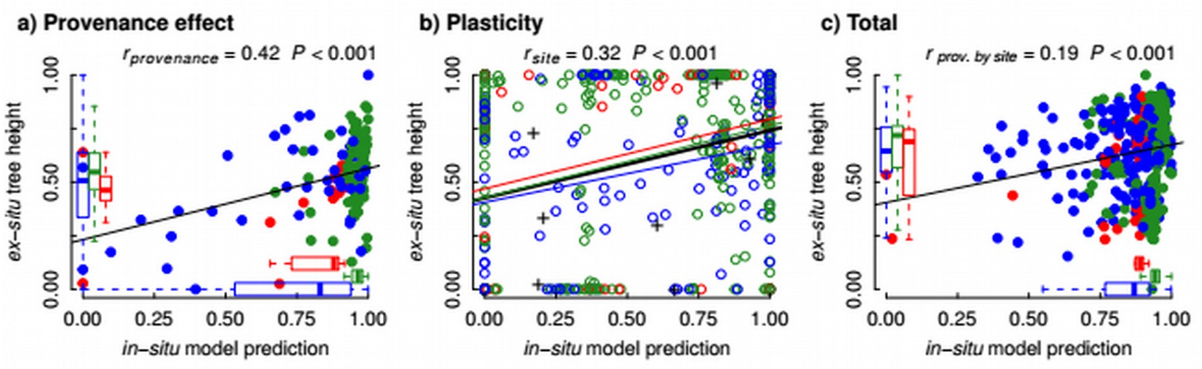

Fig S6.3 Pearson correlation coefficients between *in-situ* model predictions (calibrated on NFI) and common garden data estimates of provenance (a) and plasticity effects (b) and of the total component of tree height variation (c) across *Quercus petraea* provenances. Points represent provenance means in a) and provenance-by-site means in b) and c). Tree height differences among cold (blue), core (green) and warm provenances (red) for common garden data and *in-situ* model predictions are indicated by boxplots in a) and c). Regression lines in b) illustrate correlations for phenotypic plasticity between common garden data and *in-situ* model predictions for cold (blue), core (green), warm (red) and all provenances (black); all are significant at $P < 0.05$; crosses indicate mean site values.

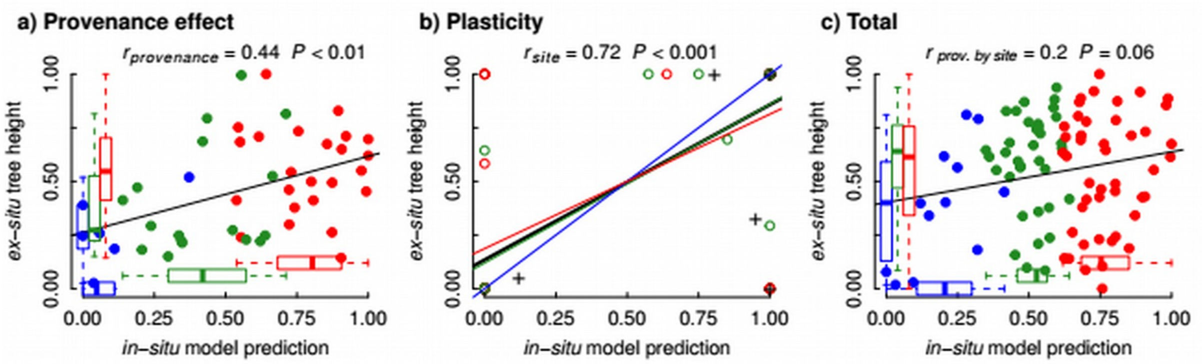

Fig S7.3 Pearson correlation coefficients between *in-situ* model predictions (calibrated on NFI) and common garden data estimates of provenance (a) and plasticity effects (b) and of the total component of tree height variation (c) across *Abies alba* provenances. Points represent provenance means in a) and provenance-by-site means in b) and c). Tree height differences among cold (blue), core (green) and warm provenances (red) for common garden data and *in-situ* model predictions are indicated by boxplots in a) and c). Regression lines in b) illustrate correlations for phenotypic plasticity between common garden data and *in-situ* model predictions for cold (blue), core (green), warm (red) and all provenances (black); all are significant at $P < 0.05$; crosses indicate mean site values.

Validation using ex-situ model predictions

In the case of validation by comparing the predictions of both models, we predicted provenance and plasticity effects, and their interaction, as a function of LTC and STC conditions in common gardens. In particular, using equation 3 (main text) we predicted the relative variation of tree height as a function of LTC_j (i.e., the provenance effect) by fixing STC_k to mean observed values across common gardens (i.e., for average climate of planting sites). Reciprocally, the relative variation of tree height as a function of STC_k (i.e., the phenotypic plasticity effect) was fitted by fixing LTC_j to mean observed values across provenances (i.e., for a mean-climate provenance). To predict plastic responses of each provenance *j*, we fitted height as a function of STC_k and the interaction term $LTC_j \times STC_k$. For this, we scaled predicted values between 0–1 independently for each provenance *j* to focus on the relative variation of height among provenances. The total component of variation was fitted as a function of LTC_j, STC_k and $LTC_j \times STC_k$, i.e. the sum of provenance and plasticity effects and their interaction. Covariates in equation 2 (main text) were fixed to constant values, i.e. *age* (the most common age in common garden data, 12-year-old trees), *BAc* (mean observed value in NFI, ~30 m^2 ha^{-1}) and their interaction with RCC_{jk} and LTC_j, respectively. Confidence intervals (SD) of predicted values along STC_k and LTC_j gradients were computed by bootstrapping, i.e., 200 model runs on 50% randomly sampled trees with replacement. In the comparison of plasticity among provenances, confidence intervals (SD) of predicted values along STC_k were computed among ‘cold’, ‘core’ and ‘warm’ provenances.